Nanotechnology **22** (2011) 505702 (7pp) doi:10.1088/0957-4484/22/50/505702

Effective mechanical properties of hexagonal boron nitride nanosheets

L Boldrin[1], F Scarpa[1,2], R Chowdhury[3] and S Adhikari[3]

[1] Advanced Composites Centre for Innovation and Science (ACCIS), University of Bristol, Bristol BS8 1TR, UK
[2] Bristol Centre for Nanoscience and Quantum Information (NSQI), University of Bristol, Bristol BS8 1UJ, UK
[3] Multidisciplinary Nanotechnology Centre, Swansea University, Swansea SA2 8PP, UK

E-mail: l.boldrin@bristol.ac.uk, f.scarpa@bristol.ac.uk, r.chowdhury@swansea.ac.uk and s.adhikari@swansea.ac.uk

Received 13 August 2011, in final form 25 October 2011
Published 23 November 2011
Online at stacks.iop.org/Nano/22/505702

Abstract
We propose an analytical formulation to extract from energy equivalence principles the equivalent thickness and in-plane mechanical properties (tensile and shear rigidity, and Poisson's ratio) of hexagonal boron nitride (h-BN) nanosheets. The model developed provides not only very good agreement with existing data available in the open literature from experimental, density functional theory (DFT) and molecular dynamics (MD) simulations, but also highlights the specific deformation mechanisms existing in boron nitride sheets, and their difference with carbon-based graphitic systems.

(Some figures may appear in colour only in the online journal)

1. Introduction

Boron nitride (BN) sheets and relative structures in hexagonal state (h-BN) have been investigated experimentally back in the 1960s [1], although a major surge of interest in boron nitride structures has stemmed from the theoretical prediction by Blase *et al* of the existence on BN tubes at the nanoscale [2]. While the open literature related to carbon nanosystems such as nanotubes and graphene is vast, less attention has been dedicated to boron nitride systems. However, BN nanostructures do exhibit electrically insulated properties, strong chemical and thermal stability but, at the same time, excellent thermal conductivities [3], and mass sensing capabilities [4]. Unlike carbon nanotubes, BN nanotubes are all semiconductors; furthermore, there is a constant wide bandgap (5.5 eV) in the BN nanotube when the diameter is greater than 9.5 Å, independent of chirality, while small BN nanotubes show interesting size-dependent electronic and magnetic properties. BNNTs are possibly the stiffest insulating nanofibres since their Young's modulus, according to both experiment ($Y = 1.1$–1.3 TPa) and theory, is approaching that of CNTs ($Y = 1.3$–1.8 TPa), while their resistance to failure can possibly surpass that of CNTs, as the experimental results from [5] seem to suggest. Few-layer h-BN thin films have been recently manufactured [6] and large h-BN areas with two to five atomic layers have been synthesized using chemical vapour deposition techniques [7]. From a mechanical perspective, the engineering constants of boron nitride sheets and nanotubes have been predicted using *ab initio* techniques by Kudin *et al* [8], 6–12 Lennard-Jones and electrostatic potentials [9] and molecular mechanics (MM) techniques by other authors [10–12]. Jiang and Guo [13] have developed an analytical MM model for boron nitride sheets and nanotubes based on the Born–Oppenheimer approximation [14] and on the 'stick-spiral' approach of Chang and Gao for carbon-based graphene and nanotubes [15]. The model developed for the BN nanostructures includes two different spiral springs or bond angle stiffness coefficients to describe the different twisting moments between boron and nitrogen atoms, respectively.

There is a strong rationale to have a compact analytical model able to describe in a closed form and high fidelity the mechanical properties of hexagonal boron nitride nanosheets, and defined by parameters corresponding to intrinsic physical deformation mechanisms. The materials designer could estimate the mechanical properties of novel types of nanocomposites based on boron nitride nanoinclusions [16, 17]

using analytical homogenization techniques typical of carbon-based nanocomposites [18, 7], when the mechanical properties of the boron nitride nanostructures are known in a closed-form fashion. Conversely, the design of novel nanomechanical (NEMS) sensors based on graphene-like structures could be greatly enhanced by the use of boron nitride nanosheets, h-BN being the thinnest 2D crystal with slightly ionic bonds [19]. To this end, the NEMS designer could take advantage of the closed-form solutions developed for graphene structures to design nanoresonators based on boron nitride nanosheets [20, 21]. However, it would be ideal to have a closed-form analytical model for h-BN nanosheets having the relatively simple formulations proper to carbon-only nanostructures, which are based on stretching and bending constants only [15, 22]. The relation between these constants and the ones from force models used in molecular mechanics is not a point clarified in the open literature [15, 23], even more for boron nitride nanostructures. This fact makes it difficult to interpret the experimental mechanical characteristics of h-BN nanosheets without a sound baseline model with physical grounding. Moreover, there is uncertainty over which equivalent thickness to use for hexagonal boron nitride configurations. The value of the thickness is an important parameter in the mechanics of solids, and the uncertainty associated with its determination produces in carbon-based nanostructures the so-called 'Yakobson's paradox', i.e. the large dispersion of data related to the Young's modulus of carbon nanotubes and graphene [24].

In this work we present an alternative analytical molecular mechanics approach for hexagonal BN sheets based on a unified method which determines an equivalent set of mechanical properties describing the BN bonds. This approach is an extension of the atomistic-continuum method developed by some of the authors for pristine [25], hydrogenated [26] and bilayer graphene [27], and the thermomechanical properties of carbon nanotubes [28]. Using this method, we will show that it is possible to describe in an analytical and compact form the in-plane mechanical properties of BN sheets (Young's and shear modulus, as well as Poisson's ratio) using only one angular stiffness and stretching coefficient, both depending analytically from the force models used (DREIDING and UFF) and the equivalent mechanical behaviour of the BN bonds. The model proposed in this work solves the shortcoming existing in other physical frameworks described above—compact set of force constants, detailed relation between force models and the deformation mechanisms of the h-BN sheets, and determination of the thickness of the boron nitride sheets. As a matter of comparison, the equivalent mechanical properties of the BN bonds are input in an hybrid atomistic–finite element (FE) model of finite-size BN sheets to obtain the stress–strain tensor coefficients and related engineering constants. We will show that the proposed analytical approach not only compares well with existing *ab initio* and MM approaches present in the open literature, but provides also an insight into the various deformation mechanisms that rule the in-plane elasticity of BN sheets and their differences from planar carbon-based nanostructures.

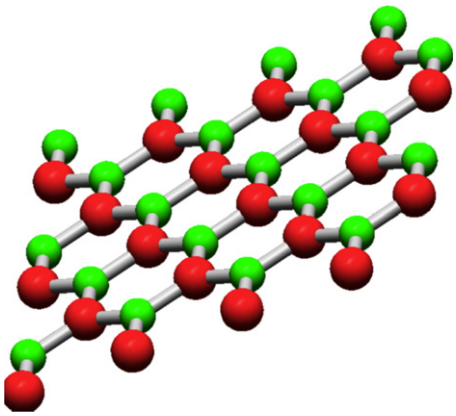

Figure 1. Example of armchair (4, 0) BN sheet. Boron atoms are in red, nitrogen atoms are in green.

2. Analytical models

2.1. BN bond

In the theoretical description that will follow, the boron nitride sheet is represented as a planar (graphite) structure (figure 1). We will use the indices I, J, K to define the positions of the boron, nitrogen and boron atoms, respectively (figure 2(a)). The equivalent mechanical behaviour of the B–N bond is represented at this stage equating the harmonic potentials with the correspondent strain energy deformations under axial, bending and torsion of a structural beam element. Differently from similar approaches used in the open literature [29], we adopt a Timoshenko beam [30] having deep shear cross-deformation behaviour as a representative beam model, to consider more realistic distributions of thickness and equilibrium length existing in C-based graphene and nanotubes [31, 25, 32]. The equivalence between the harmonic potentials and the beam strain energies for a BN bond leads to the following set of equations [32]:

$$E = \frac{4k_{IJ}r_{\mathrm{BN}}}{\pi d^2}, \qquad G = \frac{32K_{IJKL}r_{\mathrm{BN}}}{\pi d^4}, \qquad k_{IJK} = EI\frac{4+\Phi}{r_{\mathrm{BN}}(1+\Phi)}. \tag{1}$$

where E and G are the equivalent Young's and shear modulus of the material representing the B–N bond, $I = \pi d^4/32$ the polar inertia moment of the bond beam (considered having a circular cross section of diameter d, equal to the thickness, and equilibrium length r_{BN}). The k_{IJ} term in (1) represents the stretching force constant, while the bending force terms k_{IJK} and K_{IJKL} are related to the in-plane and out-of-plane rotation deformations, respectively (figure 2(a)). A condition for the validity of (1) is that in-plane and out-of-plane rotations θ and ϕ of figure 2(a) are equal, an approximation valid for small deformations and for the use of a harmonic potential [33, 31]. The shear deformation constant Φ is expressed as [25]

$$\Phi = \frac{12EI}{GA_s r_{\mathrm{BN}}^2}. \tag{2}$$

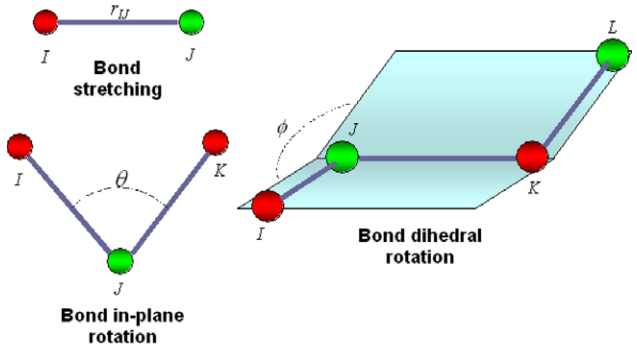

(a)

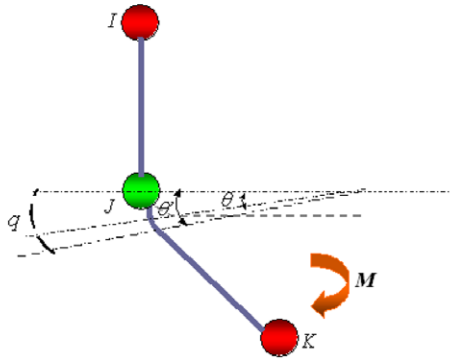

(b)

Figure 2. (a) Types of bond deformations during in-plane and out-of-plane loading and (b) hinging deformation for the IJK BN bonds.

The term Φ in (2) depends on the reduced cross section of the beam affected by the shear correction factor $A_s = A/F_s$, which is a function of the equivalent Poisson's ratio ν of the material composing the B–N bond:

$$F_s = \frac{6 + 12\nu + 6\nu^2}{7 + 12\nu + 4\nu^2}. \tag{3}$$

The expression in (3) is the Timoshenko one for the shear correction factor in beams from a circular cross section [30]. Inserting equation (3) in (1) and (2) we obtain the following nonlinear expression:

$$k_{IJK} = [\pi k_{IJ} d^2 (448\pi^2 K_{IJKL} r_{BN}^2 + 384\pi^2 K_{IJKL} r_{BN}^2 \nu + 9k_{IJ}\pi^2 d^4 \nu + 9k_{IJ}^T \pi^2 d^4)][16\pi(112\pi^2 r_{BN}^2 K_{IJKL} + 96\pi^2 r_{BN}^2 K_{IJKL}\nu + 9k_{IJ}\pi^2 d^4 \nu + 9k_{IJ}^T \pi^2 d^4)]^{-1}. \tag{4}$$

We impose the further condition that the equivalent material of the B–N bond beam behaves as isotropic, i.e. with no directional preference in its mechanical response. The isotropic condition $G = E/2/(1 + \nu)$, together with relation (4), constitutes a system of nonlinear equations which can be solved with traditional methods, such as the Marquardt algorithm. The solution of the system yields a unique value of the thickness d and Poisson's ratio ν, which depends on the specific force model used, as well as the equilibrium length r_{BN} of the BN bond.

2.2. Mechanistic models

Classical mechanistic theories for the elastic properties of single-layer graphene sheets and carbon nanotubes consider the strain energy associated with the deformation of sp^2 bonds in terms of stretching and bond angle stiffness coefficients (C_ρ and C_θ, respectively) [15]. The stretching constant C_ρ is equal to the k_{IJ} term of any force model used [25]. For the bond angle coefficient C_θ (moment per angle), we assume that, under the linear elastic regime, the BN lattice is dominated by hinging deformation. In cellular structures under general flexural/axial deformations, the relation between the change in bending angle $\Delta\theta$ and an external applied moment M with uniform distribution over the length of the bond (figure 2(b)) is provided by the following relation [34]:

$$\Delta\theta = \theta - \theta' = \int_0^q \frac{M}{EI}\,\mathrm{d}q = \frac{Mq}{EI}. \tag{5}$$

From (5), the bending angle constant can be calculated as $C_\theta = M/\Delta\theta = EI/q$, where q is the portion of the C–C bond length undergoing hinging, while the segment $r_{BN} - q$ deforms as a rigid body (figure 2(b)). Using the relations (1), the bending angle constant can be rewritten for a beam with a circular cross section: as [28]:

$$C_\theta = k_{IJ} d^2 \frac{r_{BN}}{16q}. \tag{6}$$

The constant (6) is referred to a bond only partially hinging ($q < r_{BN}$) and will therefore be defined from this point in the text as SH (semi-hinging). The rotational constant C_θ can then be used in molecular mechanics models, such as the 'stick-spiral' from Chang and Gao [15] or an energy-based method like the one from Shen and Li [23], to compute the in-plane mechanical properties of the BN sheet. In this work, we will adopt the approach from Chang and Gao to calculate the in-plane isotropic tensile rigidity $\bar{Y}$ (pressure multiplied by length), Poisson's ratio $\bar{\nu}$ and shear rigidity $\bar{G}$ [15]:

$$\bar{Y} = \frac{8\sqrt{3}C_\rho}{18 + r_{BN}^2(\frac{C_\rho}{C_\theta})} \tag{7}$$

$$\bar{\nu} = \frac{r_{BN}^2(\frac{C_\rho}{C_\theta}) - 6}{18 + r_{BN}^2(\frac{C_\rho}{C_\theta})} \tag{8}$$

$$\bar{G} = \frac{2\sqrt{3}C_\rho}{3 + 18 r_{BN}^2(\frac{C_\rho}{C_\theta})}. \tag{9}$$

Similar to other approaches [15, 23, 13], the constant C_θ is identified by known experimental or high fidelity molecular mechanics models related to the nanostructure analysed. In this work, similar to Jiang and Guo, we will use as a reference result for the identification the values for the tensile rigidity and Poisson's ratio of Kudin *et al* [8]. In sp^2 carbon systems, a pure hinging-stretching model has been often used to describe the in-plane mechanical properties of graphitic systems [35, 36]. Following [25], the rotational constant for a fully hinged bond can be expressed as $K_H = GA/r_{BN}$. The expressions for the

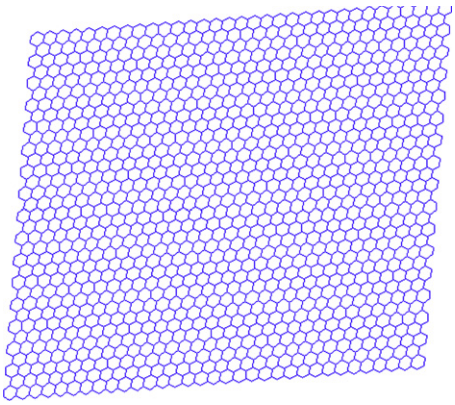

Figure 3. Finite element representation of a BN sheet made of 2278 atoms under in-plane shear loading.

tensile rigidity, Poisson's ratio and in-plane shear rigidity for a fully hinged (FH) BN nanosheet can be therefore cast as

$$\bar{Y} = \frac{4\sqrt{3}C_\rho}{3(3+\frac{C_\rho}{K_H})} \tag{10}$$

$$\bar{\nu} = \frac{1-\frac{K_H}{C_\rho}}{1+3\frac{K_H}{C_\rho}} \tag{11}$$

$$\bar{G} = \frac{\sqrt{3}C_\rho}{3(1+\frac{C_\rho}{K_H})}. \tag{12}$$

2.3. Numerical models

BN sheets and nanotubes are numerically modelled using finite element (FE) truss-like assemblies of BN bonds represented by the structural deep shear beams with the equivalent mechanical properties calculated following (1). The geometries of the BN sheets are derived from equilibrium configurations with bond angles $2\pi/3$ (figure 3).

We consider the BN sheet as an orthotropic mechanical 2D continuum with equivalent properties represented by the stress–strain second-order tensor [37]:

$$[\mathbf{C}] = \begin{bmatrix} C_{11} & C_{12} & 0 \\ C_{12} & C_{22} & 0 \\ 0 & 0 & C_{66} \end{bmatrix}. \tag{13}$$

The coefficients of the stress–strain matrix (13) are calculated from the minimization of the strain energy U of the BN sheet when mechanically loaded [38]:

$$C_{ij} = \frac{\partial^2 U}{\partial\varepsilon_i \partial\varepsilon_j}. \tag{14}$$

The strains ε_i and ε_j are imposed through periodic boundary conditions applied to rectangular sheets with 2778 atoms (figure 3). All the strains applied are equal to 1.0×10^{-4} to guarantee the limits of a linear elastic analysis.

The elastic engineering constants can be identified by the inversion of the compliance matrix [**S**] defined as [37]

$$[\mathbf{S}] = [\mathbf{C}]^{-1} = \begin{bmatrix} \frac{1}{E_1} & -\frac{\nu_{21}}{E_1} & 0 \\ -\frac{\nu_{12}}{E_2} & \frac{1}{E_2} & 0 \\ 0 & 0 & \frac{1}{G_{12}} \end{bmatrix}. \tag{15}$$

In (15), the subscripts 1 and 2 indicate the zigzag and armchair directions, respectively.

Both for the analytical and hybrid-FE models, it is necessary to identify the equivalent thickness d and Poisson's ratio ν of the BN structural bond element. We will examine now how the different force models used in this work (DREIDING and UFF) are taken into account to provide equivalent mechanical properties of the BN bonds.

3. The effect of the force model

The DREIDING force model [39] has been used by Li and Chou [40] to predict the transverse mechanical properties of single-wall BN tubes. The constants used for the BN bonds are $k_{IJ} = 4.865\times10^{-7}$ N nm^{-1} and $k_{IJK} = 6.952\times10^{-10}$ N nm rad^{-2} [39], and the torsional constant is considered as $K_{IJKL} = 6.255\times10^{-10}$ N nm rad^{-2} [40].

The UFF model [41] has been used to study the physics of a variety of nanosystems, and to develop molecular mechanics (MM) models to predict the vibrational spectroscopy of BN single-wall nanotubes [42]. It is useful to remind the equations that determine the computation of the force constants:

$$k_{IJ} = 664.12\frac{Z_I Z_J}{r_{BN}^3} \tag{16}$$

$$k_{IJK} = \beta\frac{Z_I Z_K}{r_{IK}^5} r_{IJ} r_{JK}[3r_{IJ}r_{JK}(1-\cos\theta^2) - r_{IK}\cos\theta] \tag{17}$$

$$\beta = \frac{664.12}{r_{IJ}r_{JK}} \tag{18}$$

$$r_{IK} = \sqrt{r_{IJ}^2 + r_{JK}^2 - 2r_{IJ}r_{JK}\cos\theta}. \tag{19}$$

We consider two approaches to calculate the force constants to be used in (1) and (4). Starting from the values of the MM model used in [42] ($k_{IJ} = 5.775\times10^{-7}$ N nm^{-1}, $k_{IJK} = 1.4081\times10^{-9}$ N nm rad^{-2}), it is possible to extract an equilibrium length r_{BN} from equation (16), when considering charges $Z_I = Z_B = 1.755$ and $Z_J = Z_N = 2.544$ [41]. The effective bond length r_{BN} obtained is 0.153 nm, which can then be used in (4) to determine d and ν. However, it must be noted that $r_{BN} = 0.153$ nm is larger than the values appeared in the open literature regarding BN systems, all not exceeding 0.150 nm [43, 10, 11, 3].

Another approach taken is to consider the equilibrium length r_{BN} fixed at 0.145 nm [9, 43, 13]. From (16), the stretching constant assumes the value $k_{IJ} = 6.757\times10^{-7}$ N nm. The bending constant k_{IJK} needs more attention. If we consider the angle diversion IJK (B–N–B), the product $Z_I Z_K$ is equal to 3.080 025 [41]. Using equations (17–19) for $r_{IJ} = r_{JK} = r_{BN}$, the bending constant becomes $k_{BNB} = 161.41$ kcal mol^{-1} rad^{-2}. However, when considering the

Table 1. Distribution of equilibrium length r_{BN}, thickness d, Poisson's ratio ν and bending angle constant C_θ for the various force models used.

Force model	r_{BN} (nm)	d (nm)	ν	$C_\theta \times 10^{-10}$ (N nm)	$\frac{q}{r_{BN}}$
DREIDING	0.145	0.077	−0.706	8.237	0.223
UFF	0.153	0.098	−0.437	10.877	0.318
	0.145	0.106	−0.302	9.769	0.415

N–B–N case, $Z_I Z_K = 6.471\,936$ and the bending constant becomes $k_{NBN} = 339.2$ kcal mol^{-1} rad^{-2}. We assume as a unique value for the representative BN bond in the molecular mechanics and hybrid FE-atomistic model the average between the two force constants, i.e. $k_{IJK} = 1.7389 \times 10^{-9}$ N nm rad^{-2}.

4. Results

4.1. Equivalent mechanical properties of the BN bond

Table 1 shows the results from the minimization of equation (4) and the identification of the bending angle constants C_θ for the force models used. The term C_θ has been derived from a nonlinear least-squares minimization involving the Euclidean norm of the differences between tensile rigidity and Poisson's ratio from the work of Kudin *et al*, and equations (7) and (8). A common characteristic between the DREIDING and UFF models is the identification of an *auxetic* state for the BN bond material, i.e. the Poisson's ratio is negative. A negative Poisson's ratio indicates not only a lateral expansion while the structure is subjected to tensile loading, but also an unusual equivalent large shear modulus compared to the Young's modulus of the solid representing the BN bond from a mechanical point of view. For an isotropic material, the ratio between shear and Young's modulus is $G/E = 1/2/(1+\nu)$. For the DREIDING case, $G/E \approx 1.66$, indicating that the BN bond has a higher in-plane and out-of-plane torsional stiffness than the stretching one. When considering the UFF case for $r_{BN} = 0.145$ nm, $G/E \approx 0.71$, closer to the 0.5 of sp^2 carbon bonds in graphene and nanotubes using the AMBER and the linearized Morse potential [31, 25]. Auxeticity at the nanoscale is not uncommon, having being observed in non-centrosymmetric cubic crystals [44], defective nanotubes [45–47], single-wall carbon nanotube heterojunctions and unusual systems [48–50], buckypaper with carbon nanotube entanglement and highly directional nanocomposite architectures [51, 52]. The thickness values for the UFF case are well in line with the 0.094 nm identified by Kudin *et al* using *ab initio* simulations with the PBE functional [43], with 4% and 12.7% differences against the $r_{BN} = 0.153$ nm and $r_{BN} = 0.145$ nm cases, respectively. As a matter of reference, the thickness values of the BN sheet are in line also with analogous values for graphene and carbon nanotubes, which range between 0.074 nm [53] and 0.120 nm [54].

The bond angle constant C_θ varies between 8.237×10^{-10} N nm for the DREIDING to 10.877×10^{-10} N nm for the UFF at $r_{BN} = 0.153$ nm. Jiang and Guo use two different bond angle constants C_N and C_B related to the torsional angles φ_N and φ_B within the BN lattice [13]. Using the average value $(C_N + C_B)/2$ in their closed-form solutions for the isotropic in-plane mechanical properties of a BN sheet, it is possible to obtain the same equations (7)–(9) as per Chang and Gao [15]. It is worth noticing that $(C_N + C_B)/2 = 9.935 \times 10^{-10}$ N nm, 0.4% lower than our estimate using the UFF model with $r_{BN} = 0.145$ nm. Also, the stretching constant used by Jiang and Guo (5.95×10^{-7} N nm^{-1}) is 11% lower than the one for UFF at $r_{BN} = 0.145$, but shows a discrepancy of only 3% compared to the $r_{BN} = 0.153$ nm case. From a mechanical point of view, the BN bond hinges only partially, with a percentage between 32% and 41% of the equilibrium length affected by the deformation according to the UFF model. The value of q in the BN bond is larger than the C–C sp^2 case (20% of the equilibrium length) when the AMBER force model is used [28]. However, a $q/r_{BN} = 0.22$ is observed when using the DREIDING formulation.

4.2. Tensile rigidity and Poisson's ratio

The effect of the force model can be especially observed in table 2 when considering the uniaxial properties (tensile rigidity and Poisson's ratio). The use of DREIDING leads to a lower in-plane stiffness for the analytical semi-hinged (SH) model and the hybrid atomistic-FE approach. Compared to Kudin *et al*, the SH model with DREIDING provides an 18% decrease in terms of in-plane stiffness. The lowering of the tensile rigidity is even more pronounced when considering the equivalent stiffness from the hybrid-FE model $Y = \sqrt{Y_1 Y_2}$ [32], with a decrease of 32%. Using the UFF model with the SH approach, the comparison with the *ab initio* simulations from [8] yields improved results, with a tensile rigidity reduction of 3%, and 2% lower than the one identified by Jiang and Guo [13]. These values also compare well with the 0.236 TPa nm identified by Oh using Tersoff–Brenner (TB) potentials with modified parameters in the repulsive and attractive pair potential terms for the BN interaction [11]. The use of a fully hinged (FH) approach yields stiffening effects on the tensile rigidity, varying between 16% and 21% from the DREIDING to the UFF model. However, similar results have also been observed by Oh [12] and Verma *et al*, the latter using an effective short-range potential of the Tersoff–Brenner form [55]. The hybrid atomistic-FE models provide an in-plane special orthotropic mechanical behaviour, with a degree of anisotropy Y_1/Y_2 equal to 0.98, both for the DREIDING and UFF force models. Finite-size graphitic sheets in the carbon form (graphene) do show in-plane anisotropic properties, and the degrees of anisotropy of the BN sheets appear to be in line with the ones of pristine [56–58, 25] and hydrogenated [59, 26] graphene.

Our results also compare well with other existing experimental and theoretical data available on hexagonal BN systems. It is possible to obtain from x-ray scattering measurements performed by Bosak *et al* [60] values of the tensile rigidity equal to 0.256 TPa nm (table 2), with which both our hybrid atomistic-FE and slip-spiral UFF models agree. Jager has determined by the ultrasonic method a value of $Y = 0.237$ TPa nm, which the hybrid FE-atomistic UFF

Table 2. BN graphitic layer data from the open literature and present work. Y, $\bar{\nu}$ and $\bar{G}$ are respectively the tensile rigidity, Poisson's ratio and shear rigidity of the BN nanosheet. The tensile rigidity for Verma *et al* [55] has been reported as the average between $(n, 0)$ and (n, n) sheets. The engineering constants for Bosak *et al* and Jager have been derived for $C_{11} = C_{22}$ and $C_{66} = (C_{11} - C_{12})/2$ [60, 62].

Source	Y (TPa nm)	$\bar{\nu}$	$\bar{G}$ (TPa nm)	d (nm)
[43]	0.271	0.211	0.010	0.094
[13]	0.269	0.211	0.095	—
[12]	0.322	0.161	—	0.330
[11]	0.236	0.413	—	0.330
[55]	0.348	—	0.165	0.330
[60]	0.256	0.208	0.105	0.330
[62]	0.237	0.200	0.100	0.330
FE DREIDING	0.184–0.186	0.384–0.389	0.066	0.077
FE UFF $r_{BN} = 0.153$ nm	0.198–0.202	0.400–0.405	0.072	0.098
FE UFF $r_{BN} = 0.145$ nm	0.240–0.243	0.384–0.389	0.087	0.106
FH DREIDING	0.315	−0.123	0.101	0.077
FH UFF $r_{BN} = 0.153$ nm	0.328	0.014	0.171	0.098
FH UFF $r_{BN} = 0.145$ nm	0.315	0.053	0.184	0.106
SH DREIDING $r_{BN} = 0.145$ nm	0.222	0.211	0.068	0.077
SH UFF $r_{BN} = 0.153$ nm	0.263	0.211	0.088	0.098
SH UFF $r_{BN} = 0.145$ nm	0.263	0.211	0.088	0.106

model approaches at $Y = \sqrt{Y_1 Y_2} = 0.241$ TPa nm. Also, similar to the concept of tensile rigidity, it is possible to use the membranal stiffness tensor $[\mathbf{A}] = \bar{d}[\mathbf{C}]$ for general composite and anisotropic materials [61]. The UFF hybrid atomistic-FE models with $r_{BN} = 0.145$ nm provide a value of $A_{11} = 0.286$ TPa nm, 7% greater than the value measured by Bosak *et al* [60] and 13% higher than the value detected by Jager [62]. Hamdi and Meskini using the plane-wave pseudopotential local density approximation (LDA) identify values of $A_{11} = 0.283$ TPa nm [63], which again are in line with the UFF predictions from our models.

The Poisson's ratios $\bar{\nu}$ predicted by the SH stick-spiral models are all around the value of 0.211. The limit of the fully hinged approach (FH) is evident in observing that the Poisson's ratio values, all very low, if not even negative, are outside the range of $\bar{\nu}$ present in the open literature. It is worth noticing that the experimental Poisson's ratios are between 0.200 and 0.208, only 1.4% lower than the one predicted by our analytical models. The finite-size BN sheets with orthotropic mechanical behaviour do exhibit two different in-plane Poisson's ratios (ν_{12} and ν_{21}) [57, 25]. If we consider the geometric mean $\bar{\nu} = \sqrt{\nu_{12}\nu_{21}}$ as an indicator of the Poisson's ratio for orthotropic materials [64], the corresponding Poisson's ratios range from 0.386 for the DREIDING and UFF models with $r_{BN} = 0.145$ nm, to 0.402 for the UFF model with $r_{BN} = 0.153$ nm. These values are consistent with the ones related to pristine graphene (0.397 [24]) and 0.413 from Oh [11] from TB modified potentials.

4.3. Shear rigidity

In [8], the in-plane shear modulus of BN sheets is reported as being equal to 112 GPa, with a shear rigidity of 0.010 TPa nm (table 2). These values are considerably lower than the ones predicted by our SH UFF models (0.088 TPa nm). It is worth noticing that the shear rigidity of the hybrid-FE models compares very well with the analytical stick-spiral models, with errors varying between 2.9% for the DREIDING-based models reducing to 1.1% for the UFF model with $r_{BN} = 0.145$ nm. The fully hinged analytical models tend to predict a stiffer shear behaviour, with values of shear rigidity ranging from 0.171 to 0.184 TPa nm for the two UFF-based models. Verma *et al* predict similar values at 0.165 TPa nm [55]. All our models (both analytical and hybrid-atomistic FE) compare well with the 0.09 TPa nm by Jiang and Guo [13] and the experimental results from Bosak *et al* and Jager (0.105 TPa nm and 0.100 TPa nm, respectively).

5. Conclusions

The model proposed in this work provides the following insights on the mechanics of boron nitride nanosheets:

(1) The in-plane elastic properties of h-BN sheets can be described using a single boron nitride bond mechanical model, with equivalent thickness and mechanical properties derived from the equivalence between stoichiometric potentials and mechanical strain energies related to a deep shear beam with flexural and stretching behaviour.

(2) It is possible to formulate analytically the in-plane mechanical properties of h-BN nanosheets using a stretching stiffness and only one bending angular constant, representing a global partially hinged behaviour during the uniaxial and shear deformations. Hexagonal boron nitride sheets do not appear to operate mechanically under pure stretching–hinging behaviour, contrary to carbon–carbon sp^2 bond models available in the open literature.

(3) Both the analytical (stick-spiral) and hybrid atomistic-FE approaches developed feature very good similarity with experimental, *ab initio* and other MD techniques when using the UFF model with thickness $d = 0.106$ nm and equilibrium length $r_{BN} = 0.145$ nm. The discrepancy against experimental tensile rigidity measured using x-ray diffraction is 7%, while the one versus the Poisson's ratio is only 1.4%.

The model provides a clear indication of the type of force model and thickness to be used to predict in a closed form the mechanical properties of h-BN nanosheets. Contrary to graphene structures, the model indicates that the in-plane bending deformation during uniaxial and shear loading is a physical mechanism peculiar to and dominating BN bonds.

Acknowledgment

FS is indebted to MS Cesarina Calza for the support provided while writing the manuscript.

References

[1] Lynch R W and Drickamer H G 1966 *J. Chem. Phys.* **44** 181
[2] Blase X, Rubio A, Louie S and Cohen M L 1994 *Europhys. Lett.* **28** 335
[3] Golberg D, Bando Y, Huang Y, Terao T, Mitome M, Tang C and Zhi C 2010 *ACS Nano* **4** 2979
[4] Chowdhury R and Adhikari S 2011 *IEEE Trans. Nanotechnol.* **10** 659
[5] Arenal R, Wang M-S, Xu Z, Loiseau A and Golberg D 2011 *Nanotechnology* **22** 265704
[6] Shi Y *et al* 2010 *Nano Lett.* **10** 4134
[7] Song L *et al* 2010 *Nano Lett.* **10** 3209
[8] Kudin K N, Scuseria G E and Yakobson B I 2001 *Phys. Rev.* B **64** 235406
[9] Green J F, Bolland T K and Bolland J W 1976 *J. Chem. Phys.* **64** 656
[10] Akdim B, Pachter R, Duan X and Adams W 2003 *Phys. Rev.* B **67** 245404
[11] Oh E-S 2010 *Mater. Lett.* **64** 859
[12] Oh E-S 2011 *Met. Mater. Int.* **17** 21
[13] Jiang L and Guo W 2011 *J. Mech. Phys. Solids* **59** 1204
[14] Odegard G M, Gates T S, Nicholson L M and Wise K E 2002 *Compos. Sci. Technol.* **62** 1869
[15] Chang T and Gao H 2003 *J. Mech. Phys. Solids* **51** 1059
[16] Dubrovinskaia N, Solozhenko V L, Miyajima N, Dmitriev V, Kurakevych O O and Dubrovinsky L 2007 *Appl. Phys. Lett.* **90** 101912
[17] Li T-L and Hsu S L-C 2011 *J. Appl. Polym. Sci.* **121** 916
[18] Bornert M, Bretheau T and Gilormini P 2008 *Homogenization in Mechanics of Materials* (New York: Wiley-Iste)
[19] Alem N, Erni R, Kisielowski C, Rossell M D, Gannett W and Zettl A 2009 *Phys. Rev.* B **80** 155425
[20] Wong C-L, Annamalai M, Wang Z-Q and Palaniapan M 2010 *J. Micromech. Microeng.* **20** 115029
[21] Chowdhury R, Adhikari S, Scarpa F and Friswell M I 2011 *J. Phys. D: Appl. Phys.* **44** 205401
[22] Shen L and Li J 2005 *Phys. Rev.* B **71** 035412
[23] Shen L and Li J 2004 *Phys. Rev.* B **69** 045414
[24] Huang Y, Wu J and Hwang K C 2006 *Phys. Rev.* B **74** 245413
[25] Scarpa F, Adhikari S and Phani A S 2009 *Nanotechnology* **20** 065709
[26] Scarpa F, Chowdhury R and Adhikari S 2011 *Phys. Lett.* A **375** 2071
[27] Scarpa F, Adhikari S and Chowdhury R 2010 *Phys. Lett.* A **374** 2053–7
[28] Scarpa F, Boldrin L, Peng H X, Remillat C D L and Adhikari S 2010 *Appl. Phys. Lett.* **97** 151903
[29] Tserpes K I and Papanikos P 2005 *Composites* B **36** 468
[30] Kaneko T 1974 *J. Phys. D: Appl. Phys.* **8** 1927
[31] Scarpa F and Adhikari S 2008 *J. Phys. D: Appl. Phys.* **41** 085306
[32] Scarpa F, Adhikari S, Gil A J and Remillat C D L 2010 *Nanotechnology* **21** 125702
[33] Li C and Chou T W 2003 *Phys. Rev.* B **68** 073405
[34] Masters I G and Evans K E 1996 *Compos. Struct.* **35** 403
[35] Blakslee O L *et al* 1970 *J. Appl. Phys.* **44** 3373
[36] Gillis P P 1984 *Carbon* **22** 387
[37] Hearmon R F 1961 *An Introduction to Applied Anisotropic Elasticity* (Oxford: Oxford University Press)
[38] Washizu K 1982 *Variational Methods in Elasticity and Plasticity* (Oxford: Pergamon)
[39] Mayo S L, Olafson B D and Goddard W A 1990 *J. Phys. Chem.* **94** 8897
[40] Li C and Chou T-W 2006 *J. Nanosci. Nanotechnol.* **6** 54
[41] Rappe A K, Casewit C J, Colwell K S, Goddard W A and Skiff W M 1992 *J. Am. Chem. Soc.* **114** 10024
[42] Chowdhury R, Wang C Y, Adhikari S and Scarpa F 2010 *Nanotechnology* **21** 365702
[43] Kudin K N, Scuseria G E and Yakobson B I 2001 *Phys. Rev.* B **64** 235406
[44] Grima J and Evans K 2000 *J. Mater. Sci. Lett.* **19** 1563
[45] Scarpa F, Adhikari S and Wang C Y 2009 *J. Phys. D: Appl. Phys.* **42** 142002
[46] Scarpa F, Adhikari S and Wang C Y 2010 *Int. J. Smart Nano Mater.* **1** 83
[47] Smolyanitsky A and Tewary V K 2011 *Nanotechnology* **22** 085703
[48] Scarpa F, Narojczyk J W and Wojciechowski K W 2011 *Phys. Status Solidi* b **248** 82
[49] Jindal P and Jindal V K 2006 *J. Comput. Theor. Nanosci.* **3** 148
[50] Yao Y T, Alderson A and Alderson K 2008 *Phys. Status Solidi* b **245** 2373
[51] Hall L J, Coluci V R, Galvão D S, Kozlov M E, Zhang M, Dantas S O and Baughman R H 2008 *Science* **320** 504
[52] Chen L, Liu C, Wang J, Zhang W, Hu C and Fan S 2009 *Appl. Phys. Lett.* **94** 253111
[53] Tu Z and Ou-Yang Z 2002 *Phys. Rev.* B **65** 233407
[54] Sun C Q, Bai H L, Tai B K, Li S and Jiang E Y 2003 *J. Phys. Chem.* B **107** 7544
[55] Verma V, Jindal V K and Dharamvir K 2007 *Nanotechnology* **18** 435711
[56] Reddy C D, Rajendran S and Liew K M 2005 *Int. J. Nanosci.* **4** 631
[57] Reddy C D, Rajendran S and Liew K M 2006 *Nanotechnology* **17** 864
[58] Reddy C D, Ramasubramaniam A, Shenoy V B and Zhang Y W 2009 *Appl. Phys. Lett.* **94** 101904
[59] Cadelano E, Palla P L, Giordano S and Colombo L 2010 *Phys. Rev.* B **82** 235414
[60] Bosak A, Serrano J, Krisch M, Watanabe K, Taniguchi T and Kanda H 2006 *Phys. Rev.* B **73** 041402
[61] Jones R M 1975 *Mechanics of Composite Materials* (New York: Hemisphere)
[62] Jager B 1977 *PhD Thesis* Université de Grenoble
[63] Hamdi I and Meskini N 2010 *Physica* B **405** 2785
[64] Mainprice D and Humbert M 1994 *Surv. Geophys.* **15** 575